Biphasic influence of Miz1 on neural crest development by regulating cell survival and apical adhesion complex formation in the developing neural tube

Laura Kerosuo and Marianne E. Bronner
Division of Biology and Biological Engineering, California Institute of Technology, Pasadena, CA 91125

ABSTRACT **Myc interacting zinc finger protein-1 (Miz1) is a transcription factor known to regulate cell cycle– and cell adhesion–related genes in cancer. Here we show that Miz1 also plays a critical role in neural crest development. In the chick, Miz1 is expressed throughout the neural plate and closing neural tube. Its morpholino-mediated knockdown affects neural crest precursor survival, leading to reduction of neural plate border and neural crest specifier genes *Msx-1*, *Pax7*, *FoxD3*, and *Sox10*. Of interest, Miz1 loss also causes marked reduction of adhesion molecules (*N-cadherin*, *cadherin6B*, and *α1-catenin*) with a concomitant increase of *E-cadherin* in the neural folds, likely leading to delayed and decreased neural crest emigration. Conversely, Miz1 overexpression results in up-regulation of *cadherin6B* and *FoxD3* expression in the neural folds/neural tube, leading to premature neural crest emigration and increased number of migratory crest cells. Although Miz1 loss effects cell survival and proliferation throughout the neural plate, the neural progenitor marker *Sox2* was unaffected, suggesting a neural crest–selective effect. The results suggest that Miz1 is important not only for survival of neural crest precursors, but also for maintenance of integrity of the neural folds and tube, via correct formation of the apical adhesion complex therein.**

Monitoring Editor
Denise Montell
University of California, Santa Barbara

Received: Jun 19, 2013
Revised: Nov 7, 2013
Accepted: Nov 27, 2013

INTRODUCTION

The neural crest, a multipotent stem/progenitor cell population, arises within the developing nervous system of vertebrate embryos. After induction at the neural plate border, the specification of these cells is manifested by the expression of several neural crest–specifier genes, including *FoxD3*, *Sox10*, *Ets-1*, and *Snail2*, in the dorsal neural folds. Soon thereafter, neural crest cells undergo an epithelial-to-mesenchymal transition (EMT) to detach from the neural tube and begin migration to various and often distant destinations. Subsequently, they differentiate into multiple and varied cell types, such as neurons and glia of the peripheral nervous system and melanocytes, as well as facial bone and cartilage (Sauka-Spengler and Bronner-Fraser, 2008; Kerosuo and Bronner-Fraser, 2012).

Adhesion molecules play a key role in both neural and neural crest development. N-cadherin (N-cad) expression is prominent in adherens junctions of the neural plate and neural tube, where it maintains apicobasal polarity, as well as adhesive integrity (Hatta and Takeichi, 1986; Nakagawa and Takeichi, 1995). N-cad is down-regulated from the dorsal aspect of the neural tube as neural crest cells emigrate from the neuroepithelium (Bronner-Fraser *et al.*, 1992; Nakagawa and Takeichi, 1998; Cheung *et al.*, 2005; Shoval *et al.*, 2007). *Cadherin 6B* (*Cad6B*), on the other hand, is initially expressed in the dorsal neural folds but then repressed by the transcription factor Snail2 (Inoue *et al.*, 1997; Nakagawa and Takeichi, 1998; Taneyhill *et al.*, 2007; Strobl-Mazzulla and Bronner, 2012). The expression pattern of *Cad6B* suggests a role in formation and/or maintenance of the presumptive neural crest domain within the neural folds (Nakagawa and Takeichi, 1995). *Cad6B* is indeed essential for the de-epithelialization process of premigratory neural crest cells at the onset of EMT (Park and Gumbiner, 2010), and yet its down-regulation is required for completion of EMT and proper migration of neural crest cells (Coles *et al.*, 2007). *E-cadherin* (*E-cad*) is expressed in the neuroepithelium throughout early neural development from the neural plate stage up to Hamburger and Hamilton (HH)

This article was published online ahead of print in MBoC in Press (http://www.molbiolcell.org/cgi/doi/10.1091/mbc.E13-06-0327) December 4, 2013.

Address correspondence to: Marianne E. Bronner (mbronner@caltech.edu).

Abbreviations used: Cad6B, cadherin 6B; E-cad, E-cadherin; EMT, epithelial to mesenchymal transition; HH, Hamburger Hamilton stages of chick embryonic development; Miz1, Myc interacting zinc finger protein-1; MO, morpholino; N-cad, N-cadherin; qPCR, quatitative reverse transcriptase PCR.

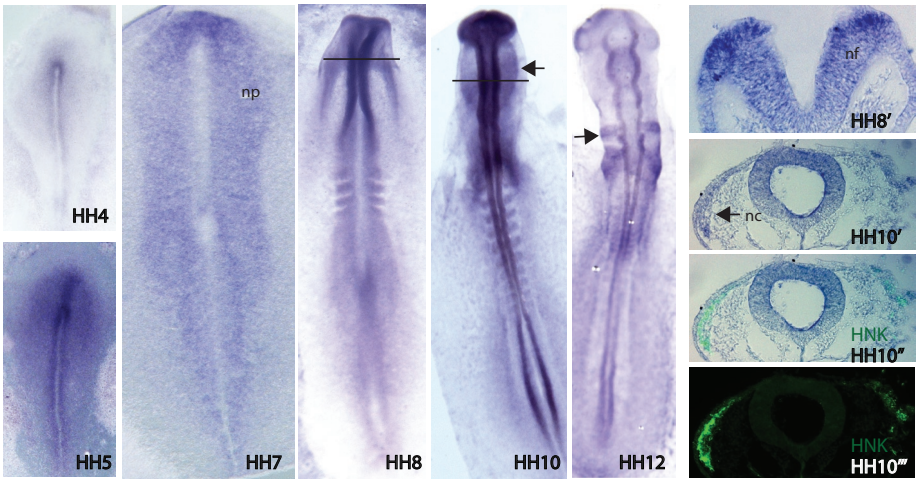

FIGURE 1: In situ hybridization showing the expression pattern of *Miz1* in the developing chicken embryo. *Miz1* expression starts during gastrulation at the neural plate at HH5, and its uniform expression continues throughout the neural plate through HH7. *Miz1* is expressed more intensely in the dorsal aspect of the neural folds at HH8, from which neural crest cells will arise (HH8′). After neurulation (HH10), *Miz1* expression continues in the neural tube, as well as in the migratory neural crest cells (black arrow) that have gone through EMT and emigrated from the tube (HH10′). At HH12, *Miz1* expression is intense in the migrating neural crest streams adjacent to rhombomere (R) 4 and R6 (black arrow). HNK immunostaining was used to mark migratory neural crest cells (HH10″). nc, neural crest; nf, neural folds; np, neural plate.

stage 11 in the chick (Dady *et al.*, 2012). Although multiple studies have focused on the mechanisms of neural crest specification in the dorsal neural folds (Kerosuo and Bronner-Fraser, 2012), the link between specification and the adhesive integrity of the neural epithelium has not been clear.

The Myc interacting zinc finger protein-1 (Miz1, also called ZBTB17) is best known for its role in transcriptional activation of cell cycle inhibitors ($p15^{ink}$, $p21^{cip}$) in cancer-associated studies (Peukert *et al.*, 1997; Staller *et al.*, 2001; Adhikary and Eilers, 2005; Phan *et al.*, 2005; Weber *et al.*, 2008). In addition, it also has been implicated in the regulation of cell adhesion by transcriptional activation of several adhesion-related genes in vitro (Gebhardt *et al.*, 2006; Herkert *et al.*, 2010). However, little is known about the expression pattern of *Miz1* or molecular mechanisms underlying its role during embryonic development in vivo. In this study, we explore the possibility that *Miz1* may represent a molecular link between neural crest specification at the neural plate border region and the adhesive changes that occur in the neuroepithelium. The results show that *Miz1* is specifically expressed in the neural ectoderm and neural crest and that its loss of function leads to severe defects in survival of the neural crest precursor pool, alterations in the adhesive complex throughout the neuroepithelium, and delay/decrease in emigration.

RESULTS

Miz1 mRNA is expressed in the neural plate and migratory neural crest

As a first step in exploring the possible function of Miz1, we examined its expression pattern in the early chick embryo during stages of neural crest formation and onset of emigration. Initiation of *Miz1* mRNA expression begins in the neural plate in the gastrulating embryo at HH5, after neural induction, as well as after the induction of the neural plate border region (Basch *et al.*, 2006; Stuhlmiller and Garcia-Castro, 2012). It is highly expressed throughout the neural plate at HH5–7 and later enhanced in the closing neural folds during neurulation (HH7–8). Expression is strongest in the dorsalmost portion of the rising neural folds at HH8, as seen in transverse section (HH8′). After neural tube closure at cranial levels (late HH8), *Miz1* continues to be expressed throughout the neural tube, with the exception of the ventralmost aspect. Emigrating neural crest cells also express *Miz1*, and immunostaining with HNK-1 antibody confirms that the *Miz1*-positive cells are migratory neural crest cells (Figure 1).

Morpholino knockdown of Miz1 affects neural crest induction at the neural plate border

Induction of the neural crest–forming region begins in the HH3 gastrula (Basch *et al.*, 2006; Stuhlmiller and Garcia-Castro, 2012), whereas expression of the neural plate border genes *Msx-1* and *Pax7* can be detected by in situ hybridization by late HH4 and is continued in the elevating neural folds throughout stages HH5–8 (Khudyakov and Bronner-Fraser, 2009). This is followed by expression of neural crest specifier genes like *FoxD3* and *Sox10* in the fully committed premigratory neural crest in the closing dorsal neural tube and emigrating cells at HH8–9 (Sauka-Spengler and Bronner-Fraser, 2008; Khudyakov and Bronner-Fraser, 2009). Because *Miz1* is expressed in the neural plate during late gastrula stages beginning at HH5, we first asked whether its knockdown affects gene expression in the neural plate border region. The results reveal a decrease in expression of *Msx-1* and *Pax7* transcripts in the neural folds at HH7 (Figure 2, A and B), observed in 81% of the embryos (n = 16) after morpholino-mediated loss of Miz1 (Figure 2D). In contrast, the neural progenitor marker *Sox2* expression does not appear to be diminished on the Miz1-treated versus control side (n = 12/12; Figure 2, F and G), although the neural tube itself appears a bit thinner.

To control for possible nonspecific effects of morpholino knockdown, we performed rescue experiments by coelectroporating Miz1 morpholino together with full-length chick Miz1, cloned into the chicken expression vector pciH2BRFP (Figure 2C). The results reveal a rescue of the expression of *Msx-1* at the neural plate border at HH7 in the majority of electroporated embryos (n = 9; 67%; Figure 2E), confirming specificity of the effect.

Loss and gain of Miz1 affect neural crest marker expression at the onset of emigration

Because Miz1 is continuously expressed during neurulation and neural crest emigration, we asked whether its knockdown also affects neural crest gene expression within the dorsal neural tube. The results show that morpholino-mediated loss of Miz1 results in a decrease in the expression of the neural crest–specifier genes *FoxD3, Sox10*, and *Ets-1* in the dorsal neuroepithelium before neural crest emigration. There are fewer *FoxD3*-expressing neural crest precursors, and the dorsal neural tube appears thinner on the morpholino (MO)-treated side compared with the contralateral control side (Figure 3, A–C). The diminution of neural crest markers was seen in 84% of the embryos after in situ hybridization (n = 32; Figure 3E). These findings were verified using quantitative PCR (qPCR) of neural tubes from HH8 embryos, which show significantly decreased

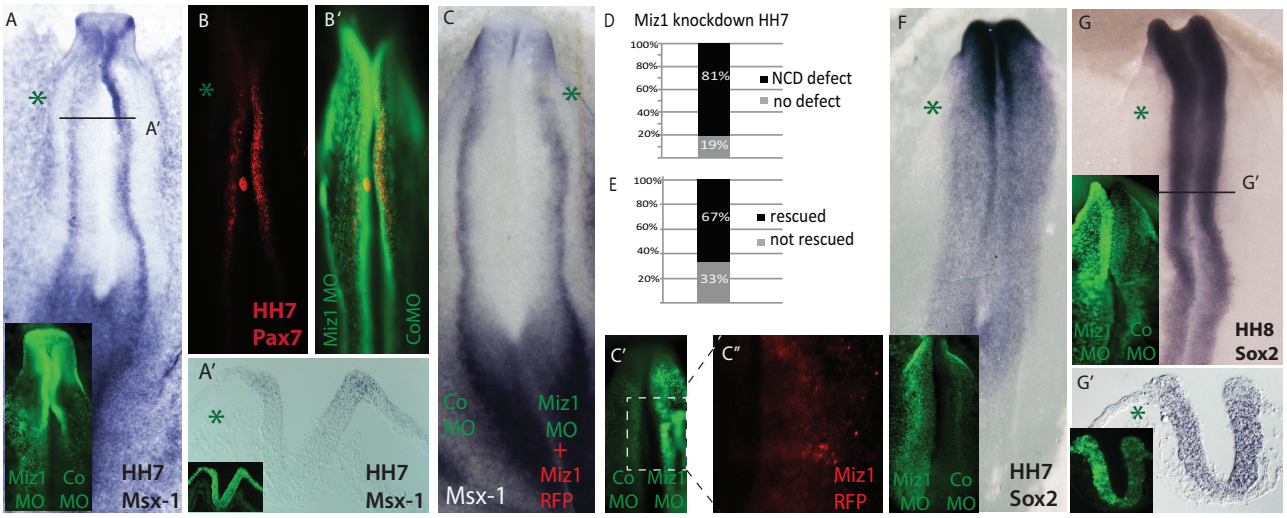

FIGURE 2: Loss of Miz1 affects the size of the prospective neural crest domain in the neural plate border. (A) Miz1 MO–mediated knockdown decreases the expression of the neural plate border marker *Msx-1* in HH7 embryos , which is also seen in the transverse section (A′). The FITC-labeled Miz1 and control MO are shown in green on respective sides. (B) Pax7 protein expression is decreased due to Miz1 knockdown in the neural plate border. (B′) Overlapping image of Pax7 and injected MOs shows Pax7 protein at the neural plate border. (C) The Miz1 loss-of-function phenotype at the neural plate border is rescued by coexpression of full-length Miz1 protein. Coelectroporation of Miz1 MO with chicken Miz1 in the PciH2BRFP vector rescues the Msx-1 expression border, as revealed by in situ hybridization at the neural plate. (C′, C″) FITC-conjugated control MO (left) and Miz1 MO (right) are shown in green, and the Miz1-RFP-positive nuclei are only visible on the rescued side on the right. (D) The loss of the neural crest domain (NCD) markers *Msx-1* and *Pax7* was seen in 81% of the embryos (E), and the phenotype was rescued by coexpression of Miz1 in 68% of the embryos. (F) *Sox2* expression in the neural plate is not significantly affected by loss of Miz1 at HH7 and (G, G′) at HH8 in the neural folds, as shown by the whole-mount figure and a transverse section of the caudal midbrain level, although the neuroepithelium appears thinner on the MO-treated side. The green asterisk marks the Miz1MO–treated side.

levels of *FoxD3* (*t* test, $p = 0.009$), *Sox10* (*t* test, $p = 0.017$), and *Msx1* (*t* test, $p = 0.021$) expression on the Miz1 MO treated-side (Figure 3D).

Conversely, overexpression of Miz1 resulted in an increase of premigratory neural crest cells in the dorsal neural tube as evaluated by the expression of *FoxD3* (Figure 3F) and *Sox10*. Overall, we detected more neural crest cells identified by an increase of cells expressing *FoxD3* or *Sox10* at HH8/9 after Miz1 overexpression in 67% of the embryos ($n = 21$; Figure 3G).

We next examined embryos at HH10–12, using *Sox10* in situ hybridization, as well as HNK immunostaining, to determine whether the effects of loss or gain of Miz1 persisted or there was recovery with time. The results suggest that the delay of neural crest cell emigration after Miz1 loss has long-lasting effects on neural crest migration, with fewer migrating neural crest cells even at HH12 (Figure 4, A and B). Of interest, we found that the effect on neural crest emigration may be a later and separate effect from the decrease in the size of the presumptive neural crest domain in the neural folds at HH7. We show that Miz1 knockdown at HH8, well after neural crest specification at the neural plate border is complete, still results in a diminution in the number of migrating neural crest cells at HH11 (Figure 4C). Conversely, overexpression of Miz1 induced premature emigration of neural crest cells from the neural tube, as well as an overall increase in the number of neural crest cells at these later stages (Figures 4, D and E).

Loss of Miz1 induces cell death and decreased proliferation

The observed thinning of the neural tube and reduction in size of the presumptive neural crest domain after loss of Miz1 (Figures 2, A′ and G′, and 3A″) led us to ask whether there might be alterations in cell survival and/or proliferation. The results show that loss of Miz1 induced a dramatic increase in apoptosis at HH7 ($n = 6/6$) as assayed by caspase immunostaining. This was further quantified in transverse sections, revealing a fivefold increase in cell death in the neural plate (NP; average 4.97, SEM 0.82, $n = 3$) and a sixfold increase in the neural crest domain (NCD) at the neural plate border (average 5.88, SEM 2.19, $n = 3$) when compared with the contralateral side of the same embryo injected with control MO and normalized to 1 (Figure 5A). We also detected a decrease in the rate of proliferation on the Miz1-morphant side in the neural plate and neural crest domain of 0.6-fold compared with the control MO side normalized to 1 (Figure 5B; NP average 0.67, SEM 0.055; NCD average 0.63, SEM 0.043, $n = 3$).

Miz1 regulates cadherins in the developing neural tube

Miz1 expression has been associated with regulation of adhesion-related molecules in the epidermis (Gebhardt *et al.*, 2006). To test whether a similar situation is in play during neural crest development, we investigated whether knockdown of Miz1 affects cell adhesion, by analyzing expression of three cadherins, N-cad, E-cad, and Cad6B, present in the developing neural tube. Immunostaining revealed a reduction of N-cad on the Miz1-morphant side throughout the neural plate at HH7 ($n = 4/5$) and the closing neural tube at HH8 ($n = 3/4$; Figure 6A). Similarly, expression Cad6B was reduced on the Miz1-morphant neural folds at HH7 ($n = 6/6$), as well as in the dorsal neural tube at HH8 ($n = 3/3$; Figure 6B). Conversely, we detected an increase of E-cad in the neural plate at HH7 ($n = 5/6$), as well as in the dorsal neural tube at HH8 ($n = 3/4$) on the Miz1-knockdown side

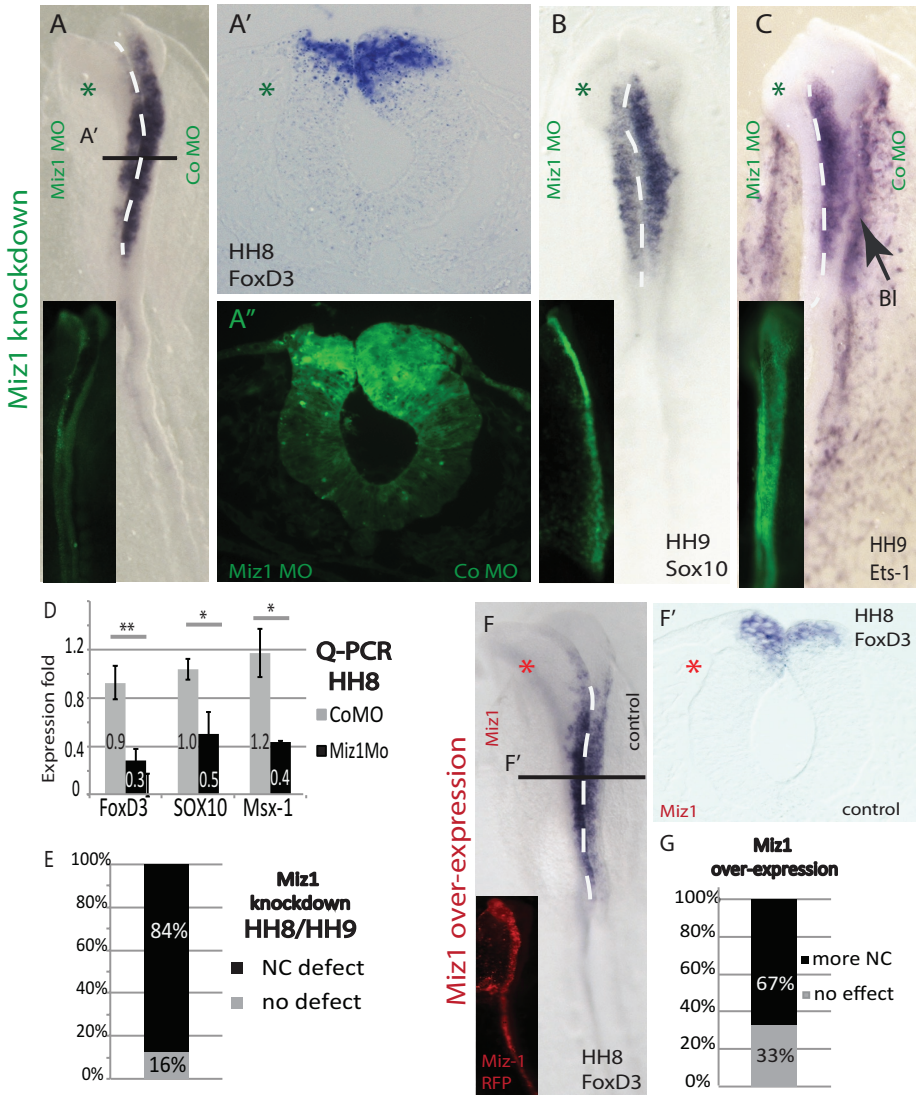

FIGURE 3: Miz1 regulates the expression of neural crest specifier genes, and its knockdown causes defects in emigration. (A) Expression of *FoxD3* is down-regulated in the dorsal neural tube at HH8 on the Miz1 MO–affected side as compared with the CoMO-treated contralateral side. (A′) A transverse section of the HH8 midbrain showing the loss of *FoxD3* (A″) as well as a thinner dorsal neural tube on the Miz1-morphant side. (B, C) The expression of *Sox10* and *Ets-1* transcripts is also decreased on the Miz1 MO–treated side of the embryo, which also shows a delay in neural crest emigration compared with the control MO side. *Ets-1* is also expressed in the extraembryonic blood islands (BI; black arrow). (D) qPCR quantification verifies the decrease of neural crest specifier genes in HH8 neural tubes due to a loss of Miz1. (E) Statistics showing the abundance of the Miz1 MO phenotype in 84% of the treated embryos. (F, F′) Overexpression of Miz1 H2B RFP at HH4 increases expression of *FoxD3* in the dorsal neural tube before neural crest emigration. Miz1-RFP is shown in red on the left side, and the empty pCAG vector was electroporated on the control side. (G) Statistics showing that increased neural crest cell marker expression was detected in 67% of the embryos. The green asterisk marks the Miz1 MO–treated and the red asterisk marks the Miz1 overexpression side.

compared with the contralateral control MO-injected side (Figure 6C). Double immunostaining confirmed that E-cad expression indeed is increased concomitant with a decrease in Cad6B in the dorsal neural tube at HH8 (Figure 6D).

Overexpression of Miz1 resulted in loss of N-cad protein on the Miz1 side at HH7 and HH8 (n = 5/5; Figure 6E) and an increase in Cad6B expression compared with the contralateral side that was injected with the empty control vector (n = 4/5; Figure 6F). We failed to detect a consistent change in the expression of E-cad after Miz1 overexpression, with the exception of a slight decrease in a portion of the neural tube visible in cross section (n = 5).

To analyze changes caused by Miz1 knockdown at the mRNA level, we performed qPCR analysis of HH8 embryos. The results revealed a significant reduction in the levels of *Cad6B* transcripts on the Miz1 morpholino-treated side (t test, p = 0.018), consistent with the immunostaining results. In contrast, there was no statistically significant change in the transcript levels of either *N-cad* or *E-cad* (Figure 6G). To further study effects on adhesion caused by Miz1 knockdown, we examined mRNA levels in the dorsal neural tubes of HH8 embryos of other adhesion molecules, *α1-catenin* or *β1-integrin*, previously shown to be Miz1 targets in other cell types (Gebhardt *et al.*, 2006). Our results show a statistically significant reduction in *α1-catenin* transcripts on the Miz1 morpholino-treated side (Figure 6G, t test, p = 0.041), whereas levels of *β1-integrin* were unchanged compared with the control side (average 1.04, SEM = 0.081).

DISCUSSION

Here we show that Miz1 is involved in the regulation of survival of developing neural tube cells and formation of apical adhesion complexes therein (Figures 5 and 6). Analysis of the expression of neural crest marker genes in the neural plate border and dorsal neural tube revealed a marked decrease in the size of the presumptive neural crest domain (Figure 2) at HH7. Of interest, neural induction appears to proceed normally after loss of Miz1, since no changes were noted in expression of the neural marker *Sox2* within the neural stem cell precursor domain in the neural plate, although there was a general thinning of the neuroepithelium consistent with the cell survival defect on both the neural crest and neural cells (Figure 2, F and G). In contrast, we noted a dramatic loss of neural plate border and neural crest–specifier genes, reflecting a diminution in the size of the neural crest domain, after knockdown of Miz1 (Figures 2 and 3). The reduction in number of *FoxD3*- and *Sox10*-expressing premigratory neural crest cells led to a delay in emigration and decrease in total number of migrating neural crest cells (Figure 4). Thus loss of neural crest cells after Miz1 knockdown may at least partially be caused by a decrease in the neural crest precursor pool caused by a critical role for Miz1 in cell survival (Figure 5). We also detected substantial changes in the adhesive properties of the entire neuroepithelium (Figure 6). The fact that levels of Cad6B transcripts and protein were significantly changed after gain or loss of Miz1 may suggest a connection between Miz1 and Cad6B that specifically affects the formation/maintenance of the neural crest domain and the transcription of

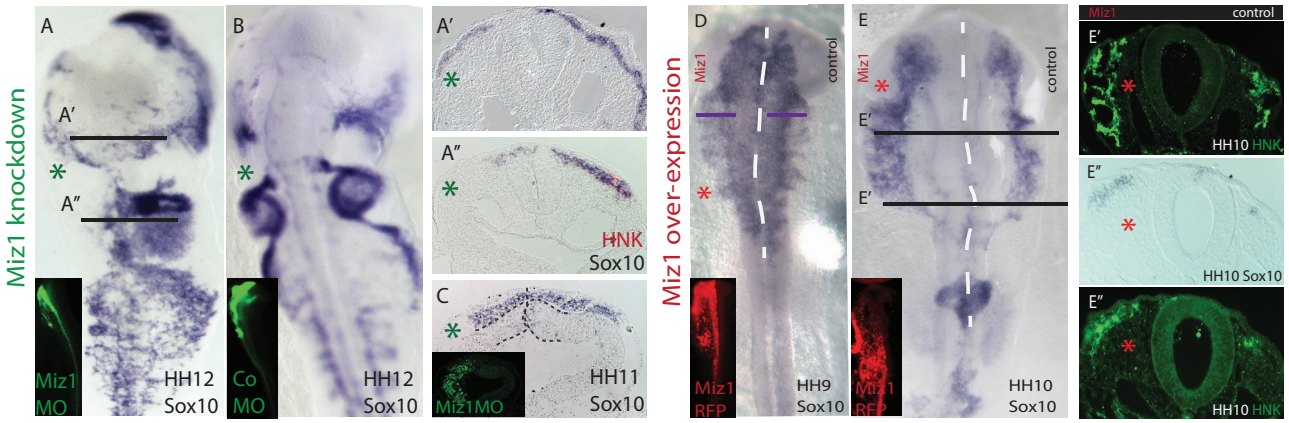

FIGURE 4: Miz is required for the proper migration of neural crest cells. (A) In situ hybridization of *Sox10* reveals that the depletion of neural crest cells caused by Miz1 knockdown at HH4 does not recover at later stages (HH12). (B) Embryos treated with CoMO on one side have normal *Sox10* expression. (A′, A″) Transverse sections of Miz1 MO–treated embryos (left) show a significant loss of migrating neural crest cells compared with the contralateral control side as assayed by *Sox10* expression and HNK immunostaining. (C) Electroporation of the Miz1 MO at HH8, into the closing neural tube well after neural crest specification is complete, still causes delayed neural crest emigration, as seen by *Sox10* in situ hybridization of a transverse midbrain section from a HH10 embryo. (D) Overexpression of Miz1 at HH4 causes an increase in the numbers of migratory neural crest cells, as shown by *Sox10* in situ hybridization in a late HH9 embryo. The equidistant purple bars on both sides demonstrate the difference between the longer lateral migration length seen on the Miz1 overexpression side vs. the control side treated with the empty pCAG vector. (E, E′, and E″) Overexpression of Miz1 increases the overall amount of the migratory neural crest cells, as shown by Sox10 in situ hybridization and HNK immunostaining in a late HH10 embryo. The green asterisk marks the Miz1 MO–treated and the red asterisk marks the Miz1 overexpression side.

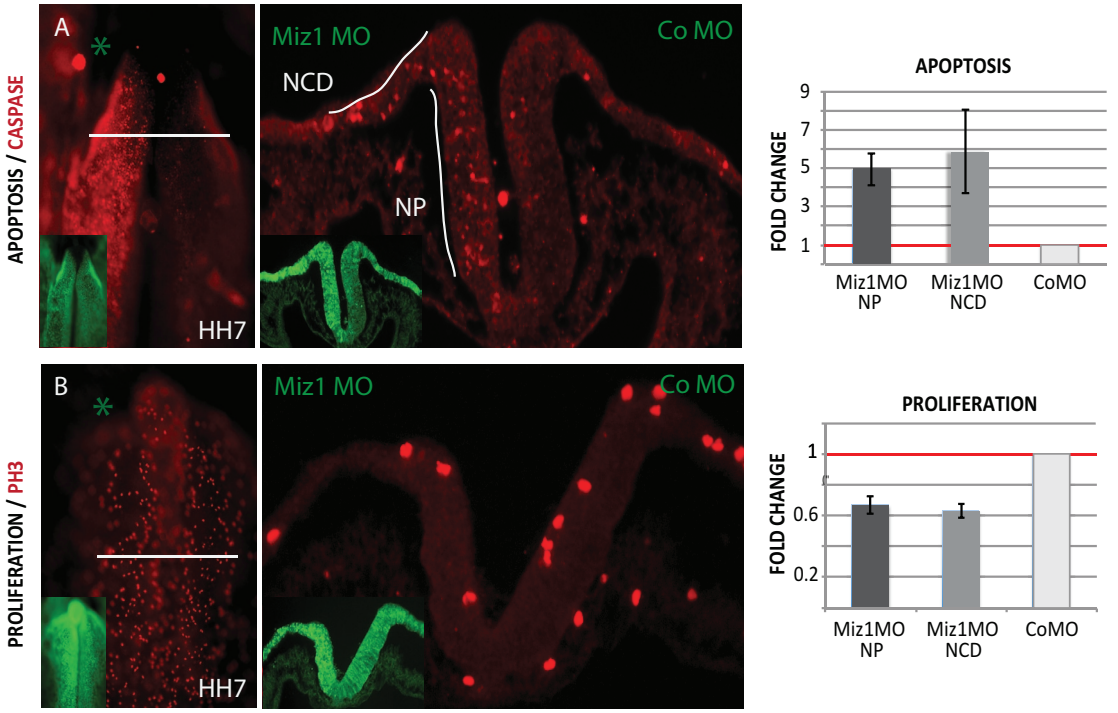

FIGURE 5: Loss of Miz1 induces apoptosis and defects proliferation in the whole neuroepithelium at HH7. (A) Immunostaining of caspase 3 shows increased apoptosis on the morphant side visible in the whole mount and transverse section of an HH7 embryo. When quantified, Miz1 Mo causes a fivefold increase in apoptosis in the neural plate (NP) and an almost sixfold increase in the neural crest domain (NCD) in the lateral neural folds as compared with the control MO–injected side, which was normalized to 1. (B) Immunostaining of the mitosis marker phospho–histone H3 shows decreased proliferation on the Miz1 MO side. The proliferation in the neural plate, as well as in the neural crest domain, was only 0.6-fold vs. the contralateral side, which was normalized to 1.

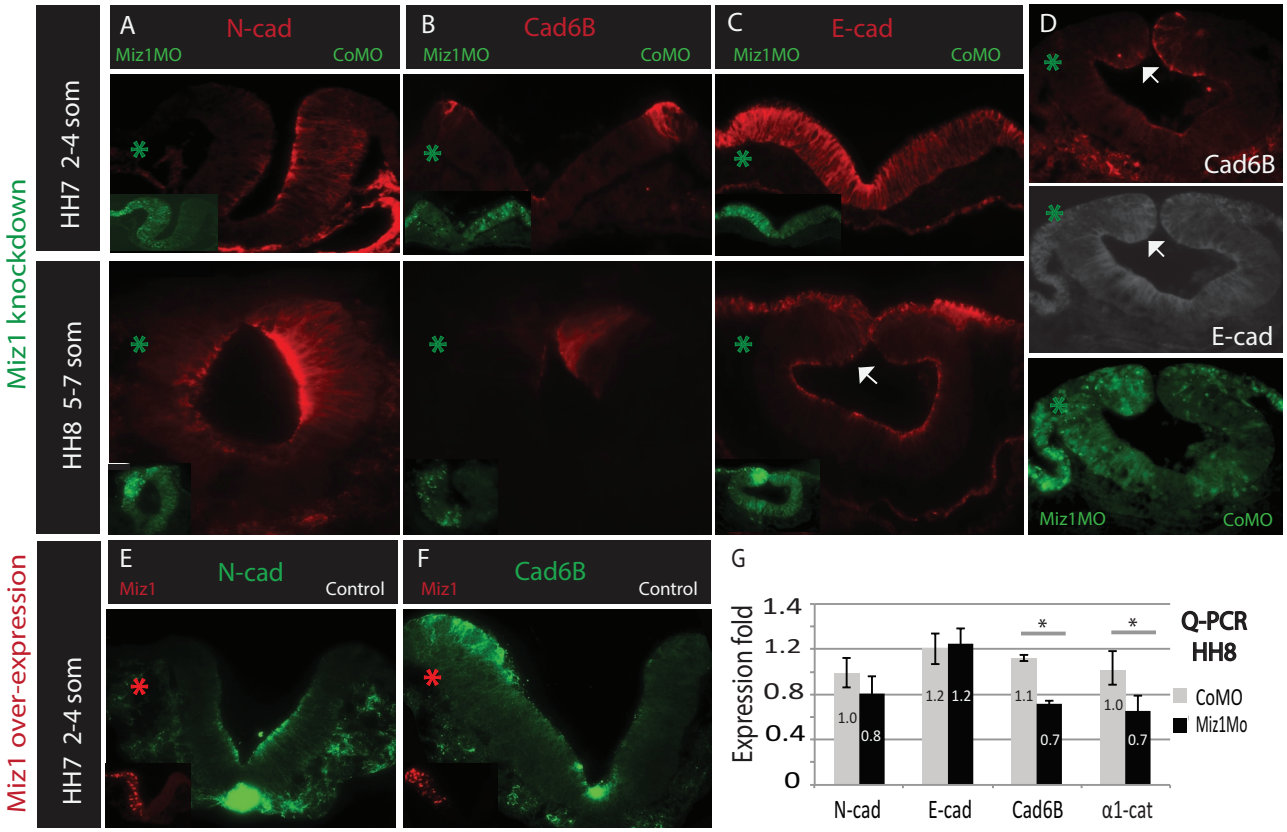

FIGURE 6: Miz1 regulates the apical adhesion complexes in the entire neuroepithelium. (A) Loss of Miz1 induces a loss of N-cad in the neural folds at HH7 and the neural tube at HH8, as shown by immunostaining. (B) Loss of Miz1 induces a loss of Cad6B in the lateral neural crest domain of the neural folds at HH7 and the dorsal neural tube at HH8, as shown by immunostaining. (C) Loss of Miz1 induces an increase of E-cad expression in the entire neural folds at HH7 and in the dorsal neural tube at HH8 (white arrow), as shown by immunostaining. (D) Double immunostaining shows decreased expression of Cad6B in the dorsal neural fold (white arrow) with concomitant increase in E-cad. (E) Overexpression of Miz1-H2BRFP decreases N-cad protein expression in the apical side of the neural folds. (F) Overexpression of Miz1-H2BRFP increases the expression of Cad6B in the neural crest domain in the lateral neural folds. (G) qPCR data show a decrease in the mRNA levels of Cad6B and a previously shown Miz1 target, α-1 catenin, which binds to cadherins and stabilizes adherens junctions. No statistically different change in the N-cadherin or E-cadherin transcript levels was observed. The green asterisk marks the Miz1 MO–treated and the red asterisk marks the Miz1 overexpression side.

the neural crest markers within. Finally, the finding that loss of Miz1 at the time of neural tube closure still causes defects in neural crest emigration (Figure 4C) suggests that Miz1 at least partially alters the EMT process independent of its effects on neural crest survival and adhesion at the neural plate border. It is interesting to note that as the neural folds elevate, the intensity of Miz1 expression increases at the dorsal tips of the closing neural tube (Figure 1, HH8′). This further suggests a potentially important function at this time that may be distinct from its earlier role.

In cancer cells and keratinocyte cultures, Miz1 regulates the expression of several adhesion-related genes and is required for maintenance of the proper polarized structure of the epidermis (Gebhardt *et al.*, 2006; Herkert *et al.*, 2010). Similarly, we noted significant changes in expression and distribution of cadherins in the developing neuroepithelium (Figure 6). Loss of Miz1 caused a reduction in N-cad protein and a concomitant increase in E-cad levels in the apical adhesion complex in the neural plate. This N-cad to E-cad switch is similar to that seen after Sip1 knockdown (Rogers *et al.*, 2013). Moreover, we found that Cad6B was decreased in the prospective "neural crest domain" at HH7 due to a loss of Miz1 and increased after its overexpression. Expression of Cad6B in the developing neural tube is essential for proper neural crest development (Nakagawa and Takeichi, 1995; Park and Gumbiner, 2010). Overall, either loss or gain of Miz1 alters the balance of the three cadherins expressed in the neuroepithelium. Together with the observed alterations in neural crest marker genes, this suggests that their correct balance is key for proper formation of the neural crest domain and subsequent emigration from the neural tube.

Another protein involved in cell–cell adhesion and previously associated with Miz1 (Gebhardt *et al.*, 2006) is α1-catenin (also called αE-catenin). It is expressed apically throughout the neuroepithelium, as well as in the migrating neural crest cells (Nakagawa and Takeichi, 1995), and thus shares an overlapping expression pattern with Miz1. Cadherins form complexes with intracellular catenins and together they comprise adherens junctions that control the apicobasal polarity of epithelial cells by tight attachment to the actin cytoskeleton. α-Catenins are linkers between the cadherin/β-catenin (or plagoblin) complexes and actin-binding proteins such as vinculin, talin, and α-actinin (Taneyhill, 2008). We observed a decrease in the expression of *α1-catenin* mRNA as well as *Cad6B* in the HH8 embryos after Miz1 knockdown, whereas the mRNA levels of *Ncad* and *Ecad* were not changed (Figure 6). In line with our results, in vitro overexpression of Cad6B in L cells induces increased expression of α1-catenin (Nakagawa and Takeichi, 1995). Similarly, overexpression of another

catenin expressed in the neural crest cells, *α2-catenin* (*or αN-catenin*), caused ectopic and increased Cad6B expression in the premigratory neural tube (Jhingory *et al.*, 2010). It is intriguing to speculate that Miz1 may be directly regulating the expression of Cad6B and/or α1-catenin, which is needed for the stabilization of both N-cad and Cad6B. Alternatively, the lack of the correct balance of N-cad/E-cad in the neural plate may cause alterations in the neural crest domain that secondarily lead to defects in Cad6B expression.

One of the major phenotypes seen after a loss of Miz1 is a dramatic decrease in cell survival throughout the neural plate, including the neural crest domain (Figure 5A). This likely contributes to the reduction of cells expressing the neural crest marker genes in the neural folds. Consistent with our findings, Miz1 protects cultured fibroblasts from tumor necrosis factor-α/JNK–induced apoptosis (Yang *et al.*, 2010). Similarly, homozygous Miz1-knockout mice die of a general failure in development at E7.5, when gastrulation is ongoing and neurulation is beginning. Lack of Miz1 also causes defects in extraembryonic tissues and massive apoptosis, as well as a lack of $p57^{kip}$, in the whole embryo (Adhikary *et al.*, 2003). However, we speculate that this function is separate from the regulation of the adhesion complexes, since the apoptosis and proliferation defect was seen throughout the neural plate, but loss of Miz1 selectively affected neural crest marker expression. Whereas neural crest marker expression was compromised, neural specification proceeded normally, as shown by the normal size of the *Sox2*-expressing neural stem cell domain (Figure 2G′). This suggests that Miz1 selectively affects neural crest precursors. This may not be surprising, given that Miz1 comes on at HH5, well after neural induction is complete, suggesting that it may have a specific role in the survival of developing neural crest cells. Intriguingly, sumoylation of Miz1 in cancer cells by interaction with Arf disrupts the transcriptional activator complex formed by Miz1 and nucleophosmin, which causes repression of multiple genes involved in cell adhesion and signal transduction. This results in weakening of cell–cell and cell–matrix interactions and induces apoptosis (Herkert *et al.*, 2010). Thus the adhesive changes caused by loss of Miz1 may be a primary defect that secondarily induces apoptosis in the neuroepithelium.

Miz1 regulates differentiation in the epidermal stem cell niche in vivo by coordinating the exit of epidermal stem cells from their niche and thus regulating the balance of keratinocyte differentiation in a manner that involves both adhesion-related changes and cell cycle regulation (Gebhardt *et al.*, 2006). In addition to adhesive changes, we also noted decreased proliferation on the Miz1-morphant side of the embryos in the neural plate (Figure 5B). Miz1 is known to regulate transcription levels of the cell cycle inhibitors—for example, $p15^{ink}$ and $p21^{cip}$ (Adhikary and Eilers, 2005)—which may explain what occurs in the neuroepithelium. Another possibility is that the extensive apoptosis we observe may be secondary due to the compromised proliferation capacity of the neuroepithelium. Finally, it is intriguing to speculate that the adhesion maintenance and proliferation may be directly connected, as transcriptional changes in cyclinD have been reported as a consequence of the cytoplasmic tail of N-cadherin acting as a transcription factor in delaminating neural crest cells (Shoval *et al.*, 2007).

In the vast majority of studies on Miz1 function, it has been shown to act as a transcriptional repressor in a complex with the c-Myc/Max oncogene duo (Adhikary and Eilers, 2005). For example, a Miz1/c-Myc complex regulates neural stem cell self-renewal in embryonic neurospheres (Kerosuo *et al.*, 2008). Despite the fact that Miz1 and c-Myc are often linked, c-Myc is not expressed in the neural plate at the time we note defects in neural crest induction (HH7). Instead, another Myc family member, N-Myc, is expressed in the neural plate (Khudyakov and Bronner-Fraser, 2009). Thus it is intriguing to speculate that Miz1 may act together with N-Myc in the developing neural tube. Consistent with this possibility, N-Myc has been shown to interact with Miz1 in cell lines of the neural crest–derived cancer neuroblastoma (Akter *et al.*, 2011). Alternatively, Miz1 may function as an independent transcriptional activator at these stages or form a repressive complex with another partner. In addition to c-Myc, Miz1 has been shown to interact with TopBP1, BCL6, Zbtb4, and p14Arf (Adhikary and Eilers, 2005; Phan *et al.*, 2005; Liu *et al.*, 2006; Weber *et al.*, 2008; Herkert *et al.*, 2010).

Similar to activation of Miz1 in the epidermis by transforming growth factor-β (TGFβ) signaling (Gebhardt *et al.*, 2006, 2007), TGFβ family members bone morphogenetic protein 4/7 (BMP4/7) are expressed at the neural plate border and critical for neural crest specification in this region. Later BMP4 is expressed in the tips of the dorsal neural folds at early HH8 and is a major neural crest inducer (Liem *et al.*, 1995). Given that BMP4 activates expression of Cad6B and RhoB and its expression is crucial for neural crest EMT (Liu and Jessell, 1998; Park and Gumbiner, 2010), Miz1 may represent a transcriptional link between BMP signaling and effects on adhesion molecules and cell survival in the developing neural tube.

In addition to its role as a transcription factor, there is some evidence that Miz1 may play other intracellular roles. In a hepatocyte cell line, for example, Miz1 is largely cytoplasmic and associated with microtubules and cholesterol metabolism; it reacts to cytoskeletal changes and translocates into the nucleus only upon microtubule depolymerization (Ziegelbauer *et al.*, 2001). Thus it is possible that the effects of Miz1 loss observed on cell adhesion molecules occur by intracellular rather than transcriptional mechanisms.

In summary, our results reveal for the first time a critical role for the transcriptional regulator Miz1 during neural crest development. Miz1 affects gene expression at two levels of the neural crest gene regulatory network—at the neural plate border/neural folds and in the emigrating bona fide neural crest cells. This leads to long-lasting alterations in migrating neural crest cell numbers. Our results reveal changes in adhesion molecules and survival of the cells throughout the entire neuroepithelium that ultimately affect the ability of the neural crest cells to properly form and emigrate from the neural tube.

MATERIALS AND METHODS

In situ hybridization

Embryos were fixed with 4% paraformaldehyde, washed with phosphate-buffered saline/0.1% Tween, dehydrated in MeOH, and stored at −20°C. The avian Miz1 probe was made by using chEST672h7 (www.chick.manchester.ac.uk), and the *Sox10*, *FoxD3*, *Msx-1*, and *Sox2* probes were made by cloning respective genes to DNA vectors from reverse transcription (RT) PCR products made by using chicken whole-embryo cDNA as template. Whole-mount in situ hybridization was performed as described (Acloque *et al.*, 2008). The digoxigenin-conjugated RNA probes were visualized by using anti–dig-AP antibody (1:2000; 11093274910; Roche Diagnostics, Mannheim, Germany) and 4-nitro blue tetrazolium chloride/5-bromo-4-chloro-3′-indolyphosphate *p*-toluidine (11383213001 and 11383221001; Roche Diagnostics). Embryos were sectioned at 12–20 μm.

Morpholino knockdown/overexpression and electroporation of chicken embryos

Fluorescein isothiocyanate (FITC)–conjugated morpholinos were purchased from Gene Tools (Philomath, OR). The Miz1 translation–blocking morpholino (AACTGGGACAGCTGCTGCAAGCCAC) was targeted to the 5′ untranslated region (UTR) 78–54 base pairs before

the ATG, and a control morpholino was designed to ensure lack of nonspecific effects from electroporation (CTGCGATGAAAAACACGGGAGCACA). The MOs were diluted to 1.5 mM concentration and electroporated together with an empty pGAG vector as carrier DNA (1 μg/μl). All the electroporations presented in this study were performed at gastrula stage (HH4) unless otherwise stated. The Miz1 morpholino/vector DNA was either injected on one side of the embryo alone with the nonelectroporated side serving as an internal control or as two-sided injections with control morpholino on the contralateral side. The electroporation was carried out as previously described (Sauka-Spengler and Barembaum, 2008). Briefly, the chicken embryos were collected on Whatman filter papers and electroporated at HH4 by using 5.3 V and five pulses (50 mA/100 mA) and incubated on individual Petri dishes (Falcon 1008 35 × 10 mm) in thin albumin until they reached the desired stage. The HH8 electroporation was performed by injecting the MO into the neural tube of four- to six-somite embryos and electroporated by using 20 V and five pulses (50 mA/100 mA).

qPCR

mRNA was isolated from HH8 embryos by using the Ambion RNAqueous-Micro Kit (Life Technologies, Grand Island, NY) by individually collecting neural tube halves from the Miz1 MO–treated and contralateral control MO–treated sides, respectively. The control embryos were treated with control MO on both sides. The results are shown as the relative expression fold of the treated side versus the control side and were analyzed using the ΔΔ*CT* method (Livak and Schmittgen, 2001). Results from three to eight individual embryos were pooled and are shown as average values. The error bars represent SEM. Primers were designed to target an exon–exon boundary, and their amplification rate was verified as linear within the margin of a ±10% amplification rate change between points in the logarithmically diluted cDNA standard curve. The following primers were used: GapdHfwd, ATCACTATCTTCCACCACCGT; GapdHrev, AGCACCACCCTTCAGATGAG; SOX10fwd, AGCCAGCAATTGAGAAGAAGG; SOX10rev, GAGGTGCGAAGAGTTGTCC; FoxD3fwd, TCTGCGAGTTCATCAGCAAC; FoxD3rev, TTCACGAAGCAGTCGTTGAG; MSX1fwd, GGAACTGTGGCAGAGAAAGG; MSX1rev, AATGGCCACAGGTTAACAGC; alpha1cateninfwd, AGCCCTCAAACCAGAAGTGGA; alpha1cateninrev, TTCTTCTGCAGGATTCCTCTG; Ncadfwd, TGAAAGGCCAATCCATGCAGA; Ncadrev, TTGTCGGCTGCTTTAAGTCCC; beta1integrinfwd, TGGAGTGAATGACACGCAGGA; beta1integrinrev, GCCCTTTCTTTGGACATTCATT; Cad6Bfwd, ACCACAGACAAGGACACACAG; Cad6Brev, GAGTATTGGTGGCTTCCACCT; Ecadfwd, CAGAGACCTTCAGCTTCAGTG; and Ecadrev, CCATCCCCGTTCACCTTG.

Immunostaining

The following primary antibodies against the indicated epitopes were used: Pax7, HNK-1 (3H5), Ncad (MNCD2), and Cad6B from the Developmental Studies Hybridoma Bank (University of Iowa, Iowa City, IA) were used in a 1:10 dilution, as well as Ecad (0.25 μg/ml; 610181; BD Biosciences, San Jose, CA), the mitosis marker phospho–histone H3 for detection of proliferation (1:500; 06-570; Upstate, Millipore, Billerica, MA), and caspase 3 for detection of apoptosis (1:300; AF835; R&D Systems, Minneapolis, MN). Embryos were fixed in 4% paraformaldehyde without saline for 15 min at room temperature, washed in 0.5 M Tris-buffered saline (TBS) buffer, pH 7.5, and blocked in TBS with 10 mM $CaCl_2$, 1.5M $NaCl_2$, 0.5% Triton, 1% dimethyl sulfoxide, and 10% goat serum. The antibodies were diluted in the blocking buffer, and whole-mount embryos were stained by incubation for 2 d in +4°C (or on sections overnight in some cases) and by using the respective Alexa secondary antibodies (Life Technologies).

Rescue experiments and overexpression

The avian Miz1 coding sequence was cloned by using the predicted Ensemble sequence ENSGALT00000039813 to make the forward primer (TTTT TTCGAA ttgaactggcctgcccagc) with a *Bst*BI site and the expressed sequence tag sequence ENSGALT00000005815 for the reverse primer (TTTT GCTAGC ttttacaccgtttccaagca) added with an *Nhe*I site. The full-length PCR product was cloned into the avian expression vector PciH2BRFP with the pGAG promoter and the nuclear red florescent protein (RFP) reporter gene separated by an internal ribosome entry site. The rescues were performed by injecting Miz1 morpholino together with the full-length chicken Miz1 H2BRFP (1 μg/μl) on one side of the embryo with control morpholino together with the empty pGAG vector on the contralateral side. The Miz-1 expression sequence starts from the coding region (ATG) and is not affected by the Miz1 morpholino, which targets the 5′ UTR upstream of the coding sequence. For overexpression, 3 μg/μl Miz1 H2BRFP in EB buffer (10mM Tris-HCl, pH 8.5) was injected and electroporated on one side of the embryo and while introducing 3 μg/μl of the empty pGAG vector into the contralateral side. All electroporations were performed at HH4.

ACKNOWLEDGMENTS

This work was supported by the Sigrid Juselius Foundation, the Foundations' Post doc Pool/Finnish Cultural Foundation, and the Ella and Georg Ehrnrooth Foundation (L.K.) and by National Institutes of Health Grant HD037105 to M.E.B.

REFERENCES

Acloque H, Wilkinson DG, Nieto MA (2008). In situ hybridization analysis of chick embryos in whole-mount and tissue sections. Methods Cell Biol 87, 169–185.

Adhikary S, Eilers M (2005). Transcriptional regulation and transformation by Myc proteins. Nat Rev Mol Cell Biol 6, 635–645.

Adhikary S, Peukert K, Karsunky H, Beuger V, Lutz W, Elsässer H-P, Möröy T, Eilers M (2003). Miz1 is required for early embryonic development during gastrulation. Mol Cell Biol 23, 7648–7657.

Akter J, Takatori A, Hossain M, Ozaki T, Nakazawa A, Ohira M, Suenaga Y, Nakagawara A (2011). Expression of NLRR3 orphan receptor gene is negatively regulated by MYCN and Miz-1, and its downregulation is associated with unfavorable outcome in neuroblastoma. Clin Cancer Res 17, 6681–6692.

Basch ML, Bronner-Fraser M, Garcia-Castro MI (2006). Specification of the neural crest occurs during gastrulation and requires Pax7. Nature 441, 218–222.

Bronner-Fraser M, Wolf JJ, Murray BA (1992). Effects of antibodies against N-cadherin and N-CAM on the cranial neural crest and neural tube. Dev Biol 153, 291–301.

Cheung M, Chaboissier M-C, Mynett A, Hirst E, Schedl A, Briscoe J (2005). The transcriptional control of trunk neural crest induction, survival, and delamination. Dev Cell 8, 179–192.

Coles EG, Taneyhill LA, Bronner-Fraser M (2007). A critical role for cadherin6B in regulating avian neural crest emigration. Dev Biol 312, 533–544.

Dady A, Blavet C, Duband J-L (2012). Timing and kinetics of E- to N-cadherin switch during neurulation in the avian embryo. Dev Dyn 241, 1333–1349.

Gebhardt A, Frye M, Herold S, Benitah S, Braun K, Samans B, Watt F, Elsässer H-P, Eilers M (2006). Myc regulates keratinocyte adhesion and differentiation via complex formation with Miz1. J Cell Biol 172, 139–149.

Gebhardt A, Kosan C, Herkert B, Möröy T, Lutz W, Eilers M, Elsässer H-P (2007). Miz1 is required for hair follicle structure and hair morphogenesis. J Cell Sci 120, 2586–2593.

Hatta K, Takeichi M (1986). Expression of N-cadherin adhesion molecules associated with early morphogenetic events in chick development. Nature 320, 447–449.

Herkert B, Dwertmann A, Herold S, Abed M, Naud J-F, Finkernagel F, Harms G, Orian A, Wanzel M, Eilers M (2010). The Arf tumor suppressor protein inhibits Miz1 to suppress cell adhesion and induce apoptosis. J Cell Biol 188, 905–918.

Inoue T, Chisaka O, Matsunami H, Takeichi M (1997). Cadherin-6 expression transiently delineates specific rhombomeres, other neural tube subdivisions, and neural crest subpopulations in mouse embryos. Dev Biol 183, 183–194.

Jhingory S, Wu CY, Taneyhill LA (2010). Novel insight into the function and regulation of alphaN-catenin by Snail2 during chick neural crest cell migration. Dev Biol 344, 896–910.

Kerosuo L, Bronner-Fraser M (2012). What is bad in cancer is good in the embryo: importance of EMT in neural crest development. Semin Cell Dev Biol 23, 320–332.

Kerosuo L, Piltti K, Fox H, Angers-Loustau A, Häyry V, Eilers M, Sariola H, Wartiovaara K (2008). Myc increases self-renewal in neural progenitor cells through Miz-1. J Cell Sci 121, 3941–3950.

Khudyakov J, Bronner-Fraser M (2009). Comprehensive spatiotemporal analysis of early chick neural crest network genes. Dev Dyn 238, 716–723.

Liem KF, Tremml G, Roelink H, Jessell TM (1995). Dorsal differentiation of neural plate cells induced by BMP-mediated signals from epidermal ectoderm. Cell 82, 969–979.

Liu JP, Jessell TM (1998). A role for rhoB in the delamination of neural crest cells from the dorsal neural tube. Development 125, 5055–5067.

Liu K, Paik JC, Wang B, Lin F-T, Lin W-C (2006). Regulation of TopBP1 oligomerization by Akt/PKB for cell survival. EMBO J 25, 4795–4807.

Livak KJ, Schmittgen TD (2001). Analysis of relative gene expression data using real-time quantitative PCR and the 2(-delta delta C(T)) method. Methods 25, 402–408.

Nakagawa S, Takeichi M (1995). Neural crest cell-cell adhesion controlled by sequential and subpopulation-specific expression of novel cadherins. Development 121, 1321–1332.

Nakagawa S, Takeichi M (1998). Neural crest emigration from the neural tube depends on regulated cadherin expression. Development 125, 2963–2971.

Park KS, Gumbiner BM (2010). Cadherin 6B induces BMP signaling and de-epithelialization during the epithelial mesenchymal transition of the neural crest. Development 137, 2691–2701.

Peukert K, Staller P, Schneider A, Carmichael G, Hänel F, Eilers M (1997). An alternative pathway for gene regulation by Myc. EMBO J 16, 5672–5686.

Phan R, Saito M, Basso K, Niu H, Dalla Favera R (2005). BCL6 interacts with the transcription factor Miz-1 to suppress the cyclin-dependent kinase inhibitor p21 and cell cycle arrest in germinal center B cells. Nat Immunol 6, 1054–1060.

Rogers CD, Saxena A, Bronner ME (2013). Sip1 mediates an E-cadherin-to-N-cadherin switch during cranial neural crest EMT. J Cell Biol 203, 835–847.

Sauka-Spengler T, Barembaum M (2008). Gain- and loss-of-function approaches in the chick embryo. Methods Cell Biol 237–256.

Sauka-Spengler T, Bronner-Fraser M (2008). A gene regulatory network orchestrates neural crest formation. Nat Rev Mol Cell Biol 9, 557–568.

Shoval I, Ludwig A, Kalcheim C (2007). Antagonistic roles of full-length N-cadherin and its soluble BMP cleavage product in neural crest delamination. Development 134, 491–501.

Staller P *et al*. (2001). Repression of p15INK4b expression by Myc through association with Miz-1. Nat Cell Biol 3, 392–399.

Strobl-Mazzulla P, Bronner M (2012). A PHD12-Snail2 repressive complex epigenetically mediates neural crest epithelial-to-mesenchymal transition. J Cell Biol 198, 999–1010.

Stuhlmiller T, Garcia-Castro MN (2012). FGF/MAPK signaling is required in the gastrula epiblast for avian neural crest induction. Development 139, 289–300.

Taneyhill L (2008). To adhere or not to adhere: the role of cadherins in neural crest development. Cell Adh Migr 2, 223–230.

Taneyhill LA, Coles EG, Bronner-Fraser M (2007). Snail2 directly represses cadherin6B during epithelial-to-mesenchymal transitions of the neural crest. Development 134, 1481–1490.

Weber A *et al*. (2008). Zbtb4 represses transcription of P21CIP1 and controls the cellular response to p53 activation. EMBO J 27, 1563–1574.

Yang Y, Do H, Tian X, Zhang C, Liu X, Dada L, Sznajder J, Liu J (2010). E3 ubiquitin ligase Mule ubiquitinates Miz1 and is required for TNFalpha-induced JNK activation. Proc Natl Acad Sci USA 107, 13444–13449.

Ziegelbauer J, Shan B, Yager D, Larabell C, Hoffmann B, Tjian R (2001). Transcription factor MIZ-1 is regulated via microtubule association. Mol Cell 8, 339–349.